As Accepted by the Astrophysical Journal

HI Absorption in the Gigamaser Galaxy TXS 2226−184 and the Relation between HI Absorption and Water Emission

G. B. Taylor[1], A. B. Peck[2,3], C. Henkel[2], H. Falcke[2], C. G. Mundell[4], C. P. O'Dea[5], S.A. Baum[5], & J. F. Gallimore[6]

ABSTRACT

We report on the discovery of HI in absorption toward the gigamaser galaxy TXS 2226−184 using the VLA. The absorption appears to consist of two components – one with a width of 125 km s^{-1}, and one broader (420 km s^{-1}), both toward the compact radio source in the nucleus of the galaxy. Based on these large velocity widths we suggest that the HI absorption is produced in the central parsecs of the galaxy, on a similar scale to that which gives rise to the water maser emission. This brings to eight the number of galaxies known to exhibit both water masers and HI absorption. We explore the relationship between these two phenomena, and present a physically motivated (but unfruitful) search for water maser emission in five radio galaxies known to exhibit strong HI absorption.

Subject headings: galaxies: active – galaxies: individual (TXS 2226−184) – galaxies: nuclei – radio lines: galaxies – masers

[1]National Radio Astronomy Observatory, P. O. Box 0, Socorro, NM 87801, USA

[2]Max-Planck-Institut für Radioastronomie, Auf dem Hügel 69, D-53121 Bonn, Germany

[3]*Current address:* Harvard Smithsonian Center for Astrophysics, SAO/SMA Project, P.O. Box 824, Hilo, HI 96721, USA

[4]Astrophysics Research Institute, Liverpool John Moores University, Twelve Quays House, Egerton Wharf, Birkenhead, CH41 1lD, UK

[5]Space Telescope Science Institute, Baltimore, MD 21218, USA

[6]Department of Physics, Bucknell University, Lewisburg, PA 17837, USA

1. Introduction

A number of studies (e.g., van Gorkom *et al.* 1989, Pihlström 2001) have shown that the rate of detection of HI absorption in galaxies is highest in Compact Symmetric Objects (CSOs) and Compact Steep Spectrum (CSS) objects. Of the theories proposed to explain this phenomenon, the existence of a circumnuclear disk or torus structure seems the most likely. In this scenario, it is the orientation and geometry of the source which increases the likelihood of detecting HI in absorption. In the CSOs and CSS objects the emission is dominated by the hot spots and lobes which are not Doppler boosted. Thus, in the CSOs we have bright symmetric emission against which to search for HI absorption on parsec scales at a large range of source inclination angles. In large sources, however, the parsec scale emission is dominated by the relativistic jets. It is much harder to see HI absorption in these sources since when the source is oriented towards us, the counter jet is deboosted and any disk which is perpendicular to the jet is at an unfavorable angle for absorption.

Water megamasers are found predominantly in Seyfert 2 (or obscured) galaxies for similar reasons (Braatz, Wilson & Henkel 1997). The masing gas is usually thought to be located in a circumnuclear accretion disk (*e.g.* NGC 4258, Miyoshi et al. 1995; NGC 1068, Greenhill & Gwinn 1997). In order for the pathlength through the disk to be long enough to obtain significant amplification, the disk must be viewed nearly edge-on. Neufeld & Maloney (1995) predict that in sources that have a molecular accretion disk sufficiently dense in the central parsec to generate stimulated emission, atomic gas should be present above and below the plane of this disk where the pressure is slightly lower, as well as at larger radii. Although this atomic gas is expected to have a temperature as high as 8000 K, resulting in very low optical depths, detection is possible if the continuum source is bright enough. Thus H_2O megamaser sources which have sufficient continuum flux at 1.4 GHz are prime candidates to search for HI absorption (see NGC 1068, Gallimore, Baum & O'Dea 1996; NGC 3079, Satoh et al. 1997).

Several symmetric radio sources which exhibit HI absorption have been studied with the VLA and the VLBA. A few of these are consistent with the parsec-scale circumnuclear torus model (*i.e.* 1946+708, Peck, Taylor & Conway 1999; PKS 2322−123, Taylor et al. 1999; Hydra A, Taylor 1996). These sources exhibit very broad (several hundred km s^{-1}) shallow systems of multiple blended lines, usually slightly redshifted with respect to the systemic velocity of the galaxy. Not all HI absorption systems are interpreted as the result of a parsec scale torus however. Another class of radio sources toward which HI absorption is seen have very distinct types of absorption systems which are also close to the systemic velocity of the galaxy. These systems are comprised of only a few strong, very narrow (3–20 km s^{-1}) lines, and vary little in FWHM or optical depth across the central parsecs of the continuum source

(*i.e.,* Cen A, Peck & Taylor 1998a). This is thought to be due to a larger, kiloparsec scale disk or dust lane in the host galaxy. In both cases, only a few sources have been well studied.

Thus both HI and H_2O can be tracers of circumnuclear material. By combining observations of both types, we are attempting to better constrain the distribution of material in the central parsecs of AGN. Our survey to date encompasses several types of radio sources (Seyfert 2, LINER, CSO, etc.) with a large range of radio powers, central masses and estimated accretion rates. The standard model of the central few parsecs should scale accordingly. It might be possible for a radio galaxy with a central mass of 10^9 $M_\odot$ to have a molecular disk of radius ∼20 pc and maser emission with apparent $\sim 10^5$ $L_\odot$ isotropic luminosity (Neufeld & Maloney 1995). Here we present a search for H_2O maser emission towards symmetric sources in which the HI absorption is thought to arise in a circumnuclear torus, and a search for HI absorption towards the H_2O gigamaser galaxy TXS 2226−184.

In §2 we describe the search for water masers toward "HI torus" sources carried out with the Effelsberg 100-m telescope, and in §3 we describe VLA observations of HI absorption toward TXS 2226−184. A discussion of our current understanding of the circumnuclear environment is presented in §4.

We assume $H_0 = 75$ km s^{-1} Mpc^{-1} and q_0=0.5 throughout.

2. H_2O Maser Observations and Results

The Effelsberg 100-m telescope[7] of the MPIfR, equipped with a dual channel K-band HEMT receiver, was used to observe five sources known to have high columns of HI in their central parsecs. The system temperature was 150–250 K on a main beam brightness temperature scale. The beam size of the telescope at 22 GHz is ∼40″. The data were obtained with an autocorrelator with 8×512 channels and a bandwidth of 80 MHz (except on July 6, 2000; see below) for each of the eight backends, leading to channel spacings of 4-5 km s^{-1}. The measurements were carried out in a dual beam switching mode with a switching frequency of 1 Hz and a beam throw of 2′ in azimuth. Pointing was checked every hour on nearby continuum sources. Linear baselines were removed from the summed spectra and we estimate the flux calibration to be accurate to ±15%. Whenever not specifically mentioned, W3(OH) (3.2 Jy; Mauersberger et al. 1988) was used for amplitude calibration. No H_2O emission was detected in any of the sources down to the rms levels indicated below. Upper limits for maser luminosities (with isotropic emission assumed here and throughout

[7]The 100-m telescope at Effelsberg is operated by the Max-Planck-Institut für Radioastronomie in Bonn.

this paper) are given in Table 1. In some cases continuum detections are reported using the entire 0.5 GHz bandwidth available to the K-band HEMT receiver.

2.1. Hydra A

Hydra A is a high-luminosity FR I radio galaxy at a redshift of $z = 0.05384$. HI absorption with a width of 80 km s^{-1} is detected in this source and thought to lie in a circumnuclear disk or torus with a scale height of <30 pc (Taylor 1996). This source was observed at 21.09908 GHz on March 17, 2000. The continuum flux density at this frequency over a 0.5 GHz wide band was 2.0±0.3 Jy. The H_2O noise level obtained with 4.4 km s^{-1} channel spacing (the channel resolution is about 20% wider) was 8 mJy for a −600 km s^{-1}<V< +580 km s^{-1} band relative to 21.09908 GHz.

2.2. PKS 2322–123

PKS 2322–123 is the central cD galaxy in the cluster Abell 2597. HI is detected on the kiloparsec scale (O'Dea *et al.* 1994), as well as on smaller scales (Taylor *et al.* 1999). On the parsec scale, two distinct HI absorption lines were detected, one narrow line (110 km s^{-1} FWHM) is seen toward the core and one of the inner jet components, and a very broad line (735 km s^{-1} FWHM) appears toward only the core. This broad line is consistent with a compact, rapidly rotating circumnuclear disk with a scale height of <20 pc (Taylor *et al.* 1999). This source was observed at 20.546 GHz ($z = 0.08220$ for the H_2O rest frequency of 22.23508 GHz) on March 18, 2000. We did not try to measure a continuum flux. Calibration at the sky frequency was obtained towards NGC 7027 (5.55 Jy according to Ott et al. 1994). With 4.6 km s^{-1} channel separation we obtained an rms noise level of 4 mJy for −1050 km s^{-1}<V< +1150 km s^{-1} relative to 20.546 GHz.

2.3. NGC 3894

NGC 3894 is a nearby (z=0.01068) elliptical galaxy with twin relativistic parsec-scale jets (Taylor, Wrobel & Vermeulen 1998). The structure of the HI detected in absorption in this source is substantially more complicated than in Hydra A or PKS 2322–123. High resolution observations (Peck & Taylor 1998b) indicate that the absorbing gas might lie in a circumnuclear torus, a large number of clouds along the line of sight to the radio continuum source, or most likely, a combination of both. This source was observed on 2000 March 19

and 2000 July 6, in the latter case with 40 MHz backends. Rms limits are 4 mJy for 2800 km s^{-1} to 4300 km s^{-1} and 6 mJy for 2050 km s^{-1} to 2800 km s^{-1} LSR in March. In July, the rms was 5 mJy for 2620 km s^{-1} to 3880 km s^{-1}. In both cases, the channel separation was 4.2 km s^{-1}.

2.4. NGC 4151

NGC 4151 is a nearby (z=0.00332; distance=16.5 Mpc) Seyfert 1.5 galaxy which has been well-studied at most wavebands. MERLIN observations indicate that the HI absorption in this source occurs only toward the core with a linewidth of 90 km s^{-1} in the strongest component. If this gas is in a toroidal structure, it must be less than 50 pc in height (Mundell *et al.* 1995). This source was the nearest target in our sample. NGC 4151 was observed on March 20, 2000. We obtained 3 mJy rms noise levels for 0 km s^{-1} to 2000 km s^{-1} LSR with a channel spacing of 4.2 km s^{-1}.

2.5. 1946+708

1946+708 is a CSO at a redshift of z=0.101. This source was initially found to exhibit HI absorption in VLA observations in 1995 (Peck, Taylor & Conway 1999). This absorption was then imaged at very high angular resolution with the Global VLBI Network, showing the region of broadest absorption (FWHM$\simeq$400 km s^{-1}) toward the core, and several narrower components toward both the approaching and receding jets. The absorbing gas in 1946+708 is thought to occur in a circumnuclear torus with an outer radius of at least 80 pc and a scale height of <10 pc. Further evidence for a torus in this source is found in free-free absorption (Peck & Taylor 2001). This source was observed with the Effelsberg 100-m telescope three times, on March 19, April 13, and July 6. As with NGC 3894, the July data were obtained with 40 MHz backends. The continuum flux was measured on April 13: 0.27$\pm$0.04 Jy at 20.19535 GHz (with a bandwidth of 0.5 GHz). With a channel separation of 4.6 km s^{-1} we obtained 2-3 mJy rms values between $-1050 < V < 1180$ km s^{-1} in March, 5 mJy between $-900 < V < 1000$ km s^{-1} in April, and 4 mJy between $-550 < V < 730$ km s^{-1} in July (all velocities with respect to the central observing frequency of 20.19535 GHz).

3. TXS 2226–184 H I Observations and Results

The observations were made with Very Large Array[8] at a center frequency of 1385 MHz on 2001 April 19 and 20. The array was in the 'B' configuration, which provided an angular resolution of $\sim 6''$. A total of 3.6 hours were obtained on source on April 19th using 32 channels across a 6.25 MHz band to provide a resolution of 43 km/s. Both right and left circular polarizations were observed. Phase and bandpass calibration was obtained by short (1 min) observations of the strong (2.1 Jy) calibrator J2246–1206 every ∼20 minutes. The data were loaded in real time and a rough reduction revealed the H I detection. For the observations on the following day the velocity resolution was doubled (to 22 km/s) at the expense of only recording in right circular polarization. A total of 2.3 hours were obtained on source.

Following standard VLA calibration practices, a continuum visibility data set and image were generated from the line data for each epoch by averaging the line-free channels. These data were then self-calibrated to remove small residual phase errors. The rms noise in the final continuum image of TXS 2226–184 is 0.10 mJy. The continuum emission from TXS 2226–184 is unresolved (size <3 kpc) and there are no other sources stronger than 0.3 mJy within one arcminute. The self-calibration solutions were then transferred to the line data. Spectral line cubes were made for TXS 2226–184 and all the sources in the field (see Fig. 1) stronger than 2 mJy simultaneously using the AIPS task IMAGR. The rms noise in a single channel from the combined data set is 0.25 mJy/beam, while in the higher spectral resolution data the rms noise in a channel is 0.66 mJy/beam. The higher noise is the result both narrower channels (by factor 0.5) and less data (factor 0.24).

In Fig. 2 we present the 43 km/s resolution spectrum of TXS 2226–184. In addition to a component with width ∼125 km/s, there appear substantial wings to the line, indicative of a broader (420 km/s) component. Two Gaussian components have been fit to the data and are drawn individually in Fig. 2 along with their sum. Parameters of the fits are given in Table 2. The higher resolution (22 km/s) spectrum is shown in Fig. 3 with the Gaussian fits overlaid.

---

[8]The National Radio Astronomy Observatory is operated by Associated Universities, Inc., under cooperative agreement with the National Science Foundation.

3.1. TXS 2226–184 Continuum Observations and Results

The continuum observations were made with Very Large Array on 2001 April 24 at C, X, U, and K bands. A total of 1 hour was used to obtain the measurements presented in Fig. 4 and Table 3. The observations at frequencies of 15 GHz and below consisted of a single scan on TXS 2226–184 of 1–3 minutes duration bracketed by a 1 minute integration on the strong calibrator J2246–1206. At 22 GHz we employed the fast switching mode using a 3 minute cycle time for 18 minutes and the nearby calibrator J2236–1433. From 1.4 to 5 GHz the spectral index, α, where $S_\nu \propto \nu^\alpha$, is $\alpha = -0.66$. Between 5 and 22 GHz the spectrum steepens to a power law of slope -0.92.

The highest resolution, obtained at 22 GHz, is $0.39 \times 0.21''$ in position angle $-12°$. At this resolution TXS 2226–184 is found to be slightly resolved with an extension along PA 145.3°. This is in good agreement with the 'A' configuration VLA image presented by Falcke *et al.* (2000) at 8.46 GHz.

4. Discussion

TXS 2226–184 contains the most luminous known H_2O megamaser with a luminosity in the 1.3 cm line of 6100 $L_\odot$ (Koekemoer et al. 1995). The water maser emission from TXS 2226–184 is fairly broad, with a FWHM of 88 km s^{-1}. Recent HST observations by Falcke et al. (2000) classify the galaxy as a spiral and reveal a dust lane cutting across the nucleus. Falcke et al. (2000) also present VLA observations at 8.4 GHz showing that the radio emission is compact ($< 1''$), symmetric, and has an axis perpendicular to the dust lane. No larger-scale diffuse emission is present to the sensitivity limits of the Northern VLA Sky Survey (NVSS) at about 2 mJy/beam (Fig. 1; Condon et al. 1998).

Although the ∼420 km s^{-1} absorption probably results from neutral material associated with the atomic and molecular torus thought to feed the active nucleus, the deeper ∼125 km s^{-1} line in TXS 2226–184 could be indicative of an interaction between the radio jet and surrounding material. The water maser emission is also fairly broad (88 km/s) in TXS 2226–184, and could likewise originate from the central torus or from a jet-cloud interaction. VLBA observations of both the H_2O emission and HI absorption could help to discriminate between these two models.

Both the H_2O megamaser emission and the HI absorption are thought to arise from the central 0.1 to 100 parsecs of the molecular and atomic torus around an AGN. In searching for these two processes, however, it is important to keep in mind that the observed flux density of the maser emission falls off with distance (although this may be less steep than the inverse

square-law if the water maser emission is amplifying a beamed nuclear continuum), while the HI absorption relies on the presence of suitably bright radio emission, but is independent of distance. Perhaps because of this difference, maser emission and HI absorption studies thus far have focused on different classes of AGN. The majority of megamaser surveys have targeted low luminosity AGN, predominantly optically selected and relatively nearby Seyferts and LINER galaxies, while the HI surveys, encompassing a much smaller number of sources but usually obtaining longer integrations, have mainly targeted powerful radio galaxies. There has been one megamaser survey directed toward FRI radio galaxies (Henkel et al. 1998) and a survey of FRII galaxies and BL Lac objects has also been made (E. Ros, A. Tarchi, priv. communication), but no detections were found and the upper limits of the two latter studies have yet to be determined.

In Table 1 we summarize the properties of all known H_2O megamasers and the HI absorption detections in these systems to date. This table illustrates a fair amount of overlap with 8/19 (42%) of the sources having both H_2O megamaser emission and HI absorption. Not all megamaser sources shown have been searched carefully for HI absorption, so the actual overlap could be somewhat larger.

Given the fairly high incidence of HI absorption in systems with H_2O megamaser emission previously reported in the literature, we carried out a moderately deep search for H_2O megamaser emission in five sources with optical depths in HI of 0.1 or more. None of these sources were detected (see Table 1 for the luminosity limits derived from the observations). The luminosity limits for the two closest sources, NGC 4151 and NGC 3894 are below those of all known H_2O megamasers, so in the case of isotropic emission we would have expected to detect those sources (see Fig. 5). For the other, more-distant, systems the luminosity limits are fairly high so it is still possible that faint H_2O megamasers reside there, or that these systems are also beamed away from us. As evident from Fig. 5, there is only a weak correlation between radio power and H_2O maser luminosity, with a Spearman's rank-order correlation coefficient of 0.465 leading to a probability that the two quantities are correlated at the 97.5% level. The HI absorbers detected so far appear to be distributed in a similar way as the megamasers without any HI absorption.

There are several possible reasons for not detecting H_2O emission from the nearby sources, even if the interpretation of the HI is correct, and a pc scale molecular disk exists within the torus, as in the scenario proposed by Neufeld & Maloney (1995) based on the prototypical source NGC 4258. First, the molecular disk is expected to be extremely thin and warped by radiation pressure (Pringle 1996), making the detection of H_2O much more dependent on the geometry and orientation of the disk than the detection of HI absorption is on the orientation of the larger torus. In some sources, the radio axis might be close to

the plane of the sky, but the regions in the warped disk which have suitable temperatures and pressures to obtain population inversion do not lie along our line of sight to a continuum source nor have a long enough path length to generate self-amplification. Another possibility is that the model wherein a molecular disk is embedded in the HI torus simply does not scale to higher powered AGN. A higher accretion rate, a stronger gravitational potential, a stronger central x-ray source, or a combination of these factors might alter the temperature and pressure of the mid-plane of the torus and thus the conditions for establishing H_2O masers is not met in these systems. Conversely, the non-detection of HI absorption in a few megamaser galaxies might indicate that the H_2O emission is the result of an interaction between the jet and a nearby molecular cloud, rather than arising in an accretion disk, as is thought to be the case in Mrk 348 (Peck *et al.* 2001, in preparation), or could possibly be the result of very high spin temperatures in the atomic part of the torus, yielding extremely low HI optical depths.

Braatz, Wilson & Henkel (1997) find a detection rate for extragalactic H_2O masers of 7.2% in Seyferts 2's and LINERs in a distance-limited sample. This is a greater success rate than we achieved in selecting systems with HI absorption, but our sample is still too small to say anything meaningful about the difference. However, the number of sources with known HI absorption is increasing dramatically thanks to new facilities at the Giant Meterwave Radio Telescope (GMRT) and Westerbork Synthesis Radio Telescope (WSRT). The detection of a torus signature in either HI or H_2O masers is of interest since it can then be followed up with VLBA studies which can provide important information about the spatial distribution and velocity field of the accreting gas and the mass of the central engine.

5. Conclusions

We report on the detection of broad HI absorption in the gigamaser galaxy TXS 2226−184. Sensitive VLBI observations are being planned in order to investigate the location and kinematics of the HI gas. It will also be of interest to learn more about the parsec-scale morphology of this exceptional object.

Among known H_2O masers the incidence of HI absorption is fairly common (>42%). Although a moderately deep survey of five radio galaxies failed to yield any new H_2O megamasers, there is still some promise to a physically motivated search. In the near future it should be possible to start with larger samples of HI absorbing systems and refine our understanding of the connection between the HI absorbers and the H_2O emitters.

We thank the referee for insightful comments on an earlier draft of the manuscript. This

research has made use of the NASA/IPAC Extragalactic Database (NED) which is operated by the Jet Propulsion Laboratory, Caltech, under contract with NASA. This research has also made use of NASA's Astrophysics Data System Abstract Service.

REFERENCES

Braatz, J. A., Wilson, A. S. & Henkel, C. 1997, ApJS, 110, 321

Braatz, J. A., Wilson, A. S. & Henkel, C. 1996, ApJS, 106, 51

Condon, J.J., Cotton, W.D., Greisen, E.W., Yin, Q.F., Perley, R.A., Taylor, G.B., & Broderick, J.J. 1998, AJ, 115, 1693

Conway, J. E. 1996 in *The Second Workshop on Gigahertz Peaked Spectrum and Compact Steep Spectrum Radio Sources*, ed. I. A. G. Snellen, R. T. Schilizzi, H. J. A. Rottgering and M. N. Bremer [Leiden Observatory], 198

Conway, J. E & Blanco, P. R. 1995 ApJ, 449, L131

Falcke, H., Wilson, A.S., Henkel, C., Brunthaler, A., & Braatz, J.A. 2000, ApJ, 530, L13

Gallimore, J. F., Baum, S. A. and O'Dea, C. P. 1996 ApJ, 464, 198

Gallimore, J. F., Baum, S. A., O'Dea, C. P., Pedlar, A. & Brinks, E. 1999, ApJ, 524, 684

van Gorkom, J. H., Knapp, G. R., Raimond, E., Faber, S. M., & Gallagher, J. S. 1986, AJ, 91, 791

van Gorkom, J. H., Knapp, G. R., Ekers, R. D., Ekers, D. D., Laing, R. A., & Polk, K. S. 1989, AJ, 97, 708

Greenhill, L. J. & Gwinn, C. R. 1997, Ap&SS, 248, 261

Greenhill, L. J., Herrnstein, J. R., Moran, J. M., Menten, K. M. & Velusamy, T. 1997, ApJ, 486, L15

Greenhill, L. J., Henkel, C., Becker, R., Wilson, T. L. & Wouterloot, J. G. A. 1995, A&A, 304, 21

Hagiwara Y., Diamond, P. J., Nakai, N. 2000, in *Proceedings of the 5th EVN Symposium* Eds. J. Conway, A. Polatidis, R.Booth & Y. Pihlström, Onsala Space Observatory, Chalmers Technical University, Gothenburg, Sweden

Henkel, C., Wang, Y. P., Falcke, H., Wilson, A. S. & Braatz, J. A. 1998, A&A, 335, 463

Koekemoer, A. M., Henkel, C., Greenhill, L.J., Dey, A., van Breugel, W., Codella, C., & Antonucci, R. 1995, Nature, 378, 697

Koribalski B., 1996, in *The Minnesota Lectures on Extragalactic Neutral Hydrogen* ASP Conf. Ser. Vol. 106, ed. Skillman E. D., [ASP: San Francisco], p.238

Mauersberger, R., Wilson, T. L. & Henkel, C. 1988, A&A 201, 123

Miyoshi, M., Moran, J., Herrnstein, J., Greenhill, L., Nakai, N., Diamond, P. & Inoue, M. 1995, Nature, 373, 127

Mundell, C. G., Pedlar, A., Baum, S. A., O'Dea, C. P., Gallimore, J. F., & Brinks, E. 1995, MNRAS, 272, 355

Neufeld, D. A. & Maloney, P. R. 1995, ApJ, 447, L17

1994, ApJ, 436, 669

Ott, M., Whiteoak. J. B., Henkel, C. & Wielebinski, R. 2001, A&A, 372, 463

Ott, M., Witzel, A., Quirrenbach, A., Krichbaum, T. P., Standke, K. J., Schalinski, C. J. & Hummel, C. A. 1994, A&A 284, 331

Peck, A. B. & Taylor, G. B. 1998a, BAAS, 193, 620

Peck, A. B., & Taylor, G. B. 1998b, ApJ, 502, L23

Peck, A. B., Taylor, G. B. & Conway, J. E. 1999, ApJ, 521, 103

Peck, A. B., & Taylor, G. B. 2001, ApJ, 554, L147

Pihlström, Y.M., Conway, J.E., Booth, R.S., Diamond, P.J. &Koribalski, B.S. 2000 A&A, 357, 7

Pihlström, Y.M. 2001, Ph.D. Thesis, Chalmers University

Pringle, J. E. 1996, MNRAS, 281, 357

Sawada-Satoh, S., Inoue, M., Shibata, K. M., Kameno, S., Migenes, V., Nakai, N. & Diamond, P. J. 2000, PASJ, 52, 421

Satoh, S., Inoue, M., Nakai, N., Shibata, K. M., Kameno, S., Migenes, V., Diamond, P. J. 1997, in *The Central Regions of the Galaxy and Galaxies*, IAU Symposium 184, 208

Taylor, G. B. 1996, ApJ, 470, 394

Taylor, G. B., Wrobel, J. M., & Vermeulen, R. C. 1998, ApJ, 498, 619

Taylor, G. B., O'Dea, C. P., Peck, A. B. & Koekemoer, A. M. 1999, ApJ, 512, L27

Table 1. Megamaser and HI Detection Summary

Megamaser Source	Host Galaxy •	Isotropic Lum. ($L_\odot$)	H_2O FWHM (km s^{-1})	H_2O V_{LSR} (km s^{-1})	Maser Ref.	Isotropic $P_{1.4GHz}$ (W Hz^{-1})	Peak HI Opt. Depth (τ)	Peak HI FWHM (km s^{-1})	HI ref.
Circinus	Sy2	24	1	274–562	1	6.8×10^{21}	···	∼180	2
ESO 103-G35	Sy1/2	360	8	4073	1	···	···	···	···
IC 2560	Sy2	130	25	2919	1	5.6×10^{21}	···	···	···
IC 1481	L	320	2	6235–6237	1	2.9×10^{22}	···	···	···
Mrk 1	Sy2	64	3 – 6	4868–4869	1	3.8×10^{22}	···	···	···
Mrk 348	Sy2	450	133	4610–4678	3	1.4×10^{23}	<0.004		4
Mrk 1210	Sy2	99	0.8 – 11	4213–4314	1	4.2×10^{22}	···	···	···
NGC 1052	L/Sy2	140	80 – 120	1605–1668	1	4.0×10^{22}	0.021	35	5
NGC 1068	Sy1/2	170		800–1500	1	1.4×10^{23}	0.078	161	4
NGC 1386	Sy2	120	4	969	1	6.1×10^{20}	···	···	···
NGC 2639	Sy1.9	71	1 – 7	3300–3323	1	2.6×10^{22}	<0.003		4
NGC 3079	L/Sy2	520	10	926–1190	1,6	2.3×10^{22}	0.8	133	4,6
NGC 3735	Sy2	12	1.4–3	2262–2268	7	1.3×10^{22}	···	···	···
NGC 4258	L/Sy1.9	85	1 – 7	-365–1460	1,8	3.6×10^{21}	<1.4	···	9
NGC 4945	Sy2	57	3	694	1	4.4×10^{22}	0.29	∼250	10
NGC 5347	Sy2	32	15	2376–2401	1	6.5×10^{20}	···	···	···
NGC 5506	Sy1.9	61	0.7 – 6	1731–1821	1	2.5×10^{21}	0.109	95	4
NGC 5793	Sy2	125	1.3, 14	3190–3677	11	3.0×10^{23}	3	16, 50	12
TXS 2226-184	E/S0	6100	88	7570	1	8.7×10^{22}	0.1	125, 418	13
HI Torus Source	Host Galaxy	3σ H_2O Upper lim. (mJy)	Lum. limit† ($L_\odot$)	V_{LSR} Searched* (km s^{-1})	Maser Ref.	Isotropic $P_{1.4GHz}$ (W Hz^{-1})	Peak HI Opt. Depth (τ)	Peak HI FWHM (km s^{-1})	HI ref.
Hydra A	E	13	<140	15552–16732	13	2.3×10^{26}	0.99	80	14
PKS 2322-123	E	12	<310	23610–25811	13	2.5×10^{25}	0.3,0.6	735, 110	15
NGC 3894	E	12	< 5	2050–4300	13	8.7×10^{22}	0.1	80	16
NGC 4151	Sy1.5	9	<0.6	0–2000	13	7.0×10^{21}	0.23	90	17
1946+708	E	12	<470	29250–31480	13	2.0×10^{25}	0.1	375	18

Note. — References: (1) Braatz et al 1996 and references therein, (2) Koribalski 1996, (3) Falcke *et al.* 2000, (4) Gallimore et al 1999, (5) van Gorkom, *et al.* 1986, (6) Sawada-Satoh *et al.* 2000, (7) Greenhill *et al.* 1997, (8) Greenhill *et al.* 1995, (9) Mundell *et al.* in preparation, (10) Ott *et al.* 2001, (11) Hagiwara *et al.* 2000, (12) Pihlström *et al.* 2000, (13) this paper, (14) Taylor 1996, (15) Taylor *et al.* 1999, (16) Peck & Taylor 1998b, (17) Mundell *et al.* 1995, (18) Peck, Taylor & Conway 1999

• Sy=Seyfert, L=LINER, E=Elliptical.

† calculated assuming a linewidth of 10 km s^{-1}.

* optical velocity convention (cz).

TABLE 2

TXS 2226-184 HI COLUMN DENSITIES

Component	$S_{1.4\mathrm{GHz}}$ (mJy)	S_{line} (mJy)	V (km s^{-1})	ΔV (km s^{-1})	τ	N_{H} (cm^{-2})
(1)	(2)	(3)	(4)	(5)	(6)	(7)
narrow	73.5	12.3 ± 0.98	7491 ± 3	125 ± 10	0.183	3.3×10^{23}
broad	73.5	5.6 ± 0.74	7454 ± 18	418 ± 72	0.079	4.8×10^{23}

NOTES TO TABLE 2

Col.(1).—Component name. Col.(2).—Continuum flux density at 1.4 GHz in mJy. Col.(3).—Depth of the line in mJy. Col.(4).—Central velocity (cz) in km s^{-1}. Col.(5).—FWHM in velocity in km s^{-1}. Col.(6).—Optical depth, assuming a continuum source covering factor of unity. Col.(7).—The column density in units of cm^{-2} calculated assuming a spin temperature of 8000 K (Conway & Blanco 1995). If the HI absorption results from gas outside the nuclear region then a more reasonable assumption for the spin temperature would be 100 K, reducing the column densities quoted here by a factor of 80.

TABLE 3

CONTINUUM OBSERVATIONS

ν (GHz)	S_{VLA} (mJy)	time (min)	$\Delta\nu$ (MHz)
1.385	73.3 ± 2.2	350	5
4.860	32.2 ± 0.98	1.4	50
8.460	20.0 ± 0.60	0.8	50
14.940	11.7 ± 0.38	2.0	50
22.460	7.87 ± 0.41	10.2	50

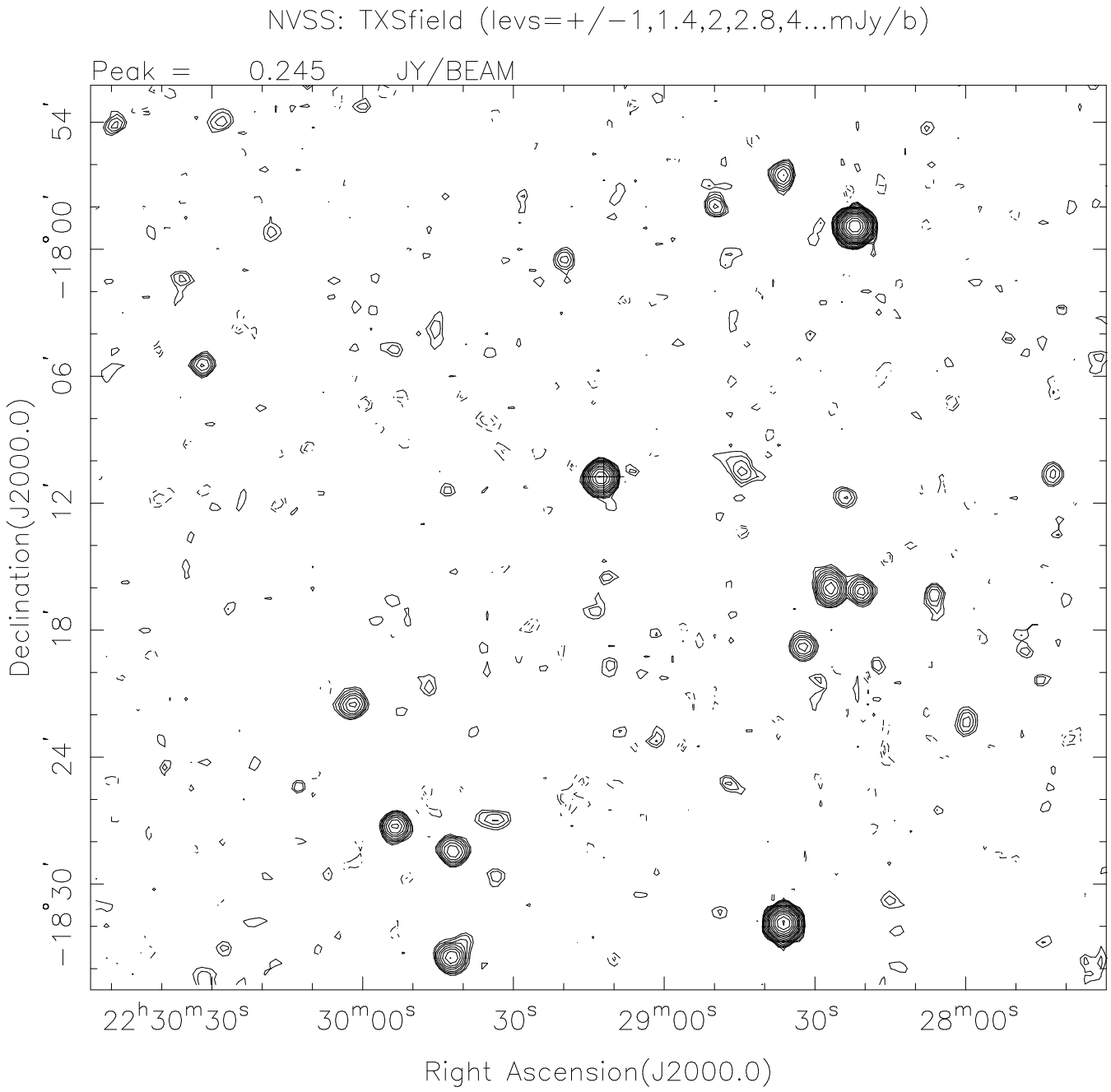

Fig. 1.— The NVSS (Northern VLA Sky Survey) image from Condon et al. 1998. Spatial resolution is 45″. Contours are drawn at −1, 1, 1.4, 2, ..., 181 mJy/beam by $\sqrt{2}$ intervals with negative contours shown dashed. The cross marks the position of TXS 2226−184.

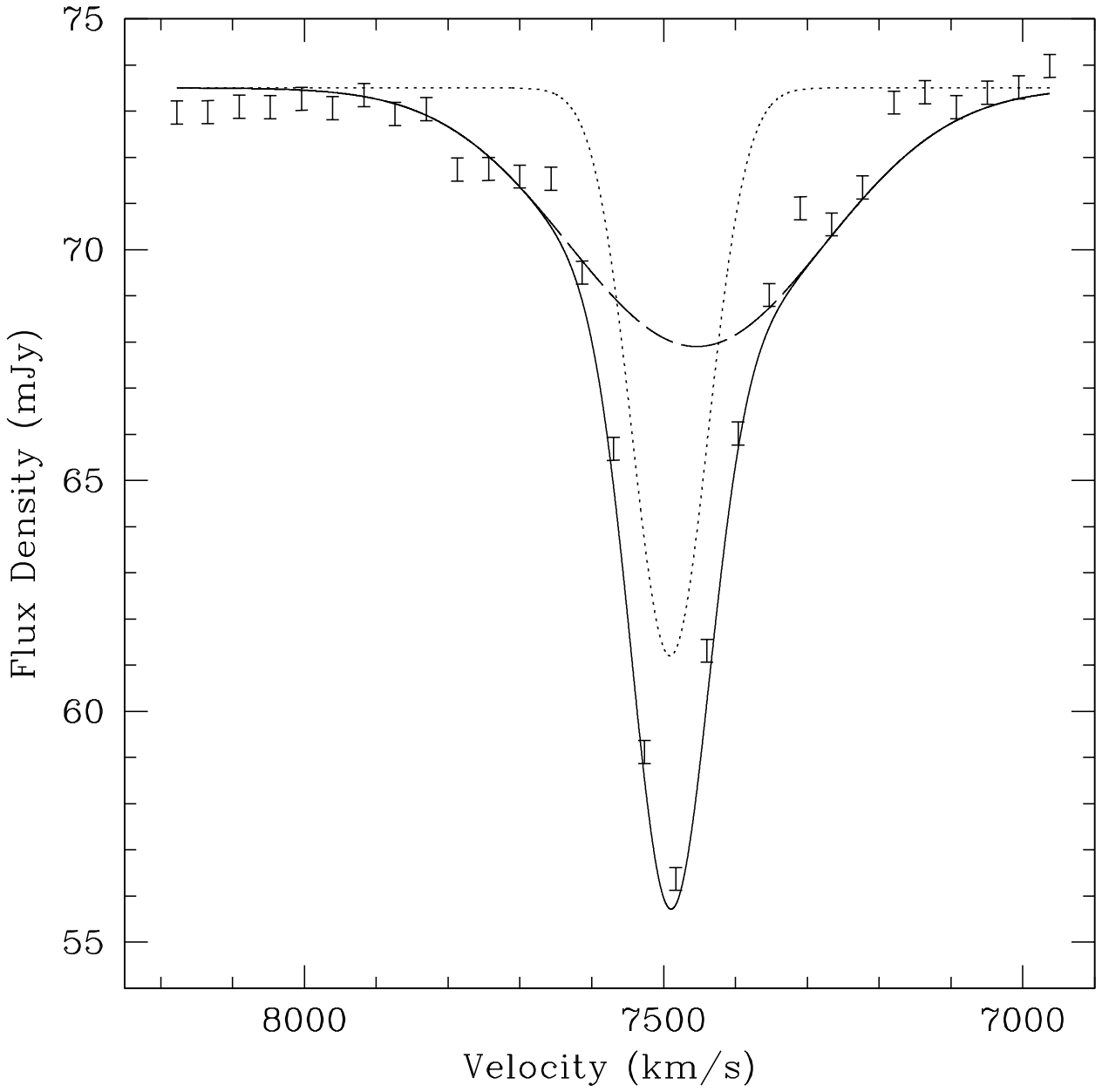

Fig. 2.— The low resolution H I spectrum towards TXS 2226−184 derived from combined observations on 2001 April 19 and 20. The velocity frame is LSR (Local Standard of Rest) and the velocity resolution is 43 km s^{-1}. The solid line represents the best fit of two Gaussians (dotted and long-dash lines) to the data.

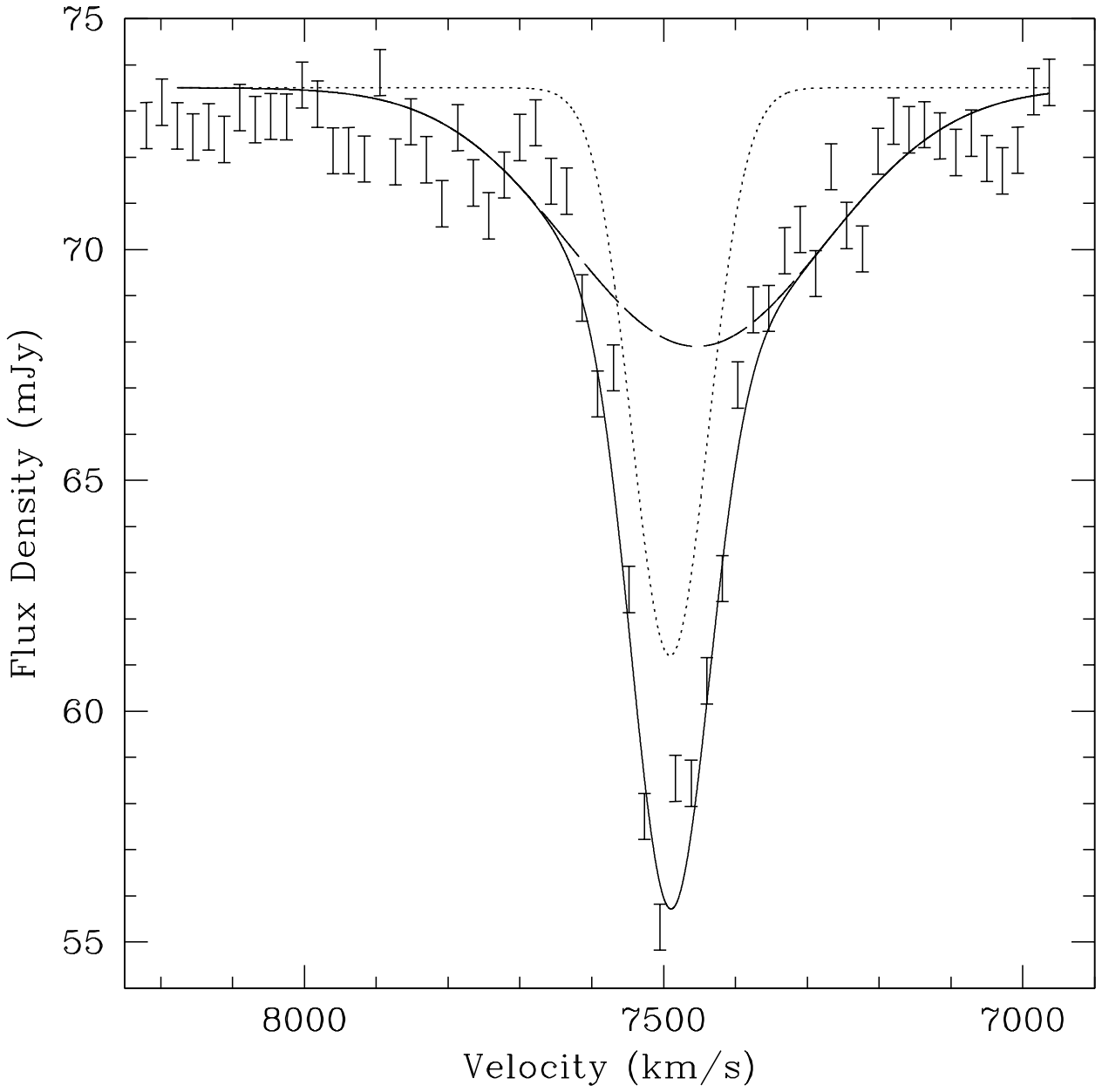

Fig. 3.— The high resolution H I spectrum towards TXS 2226−184 derived from observations on 2001 April 20. The velocity frame used is LSR and the velocity resolution is 22 km s^{-1}. The solid line represents the best fit of two Gaussians (dotted and long-dash lines) to the data.

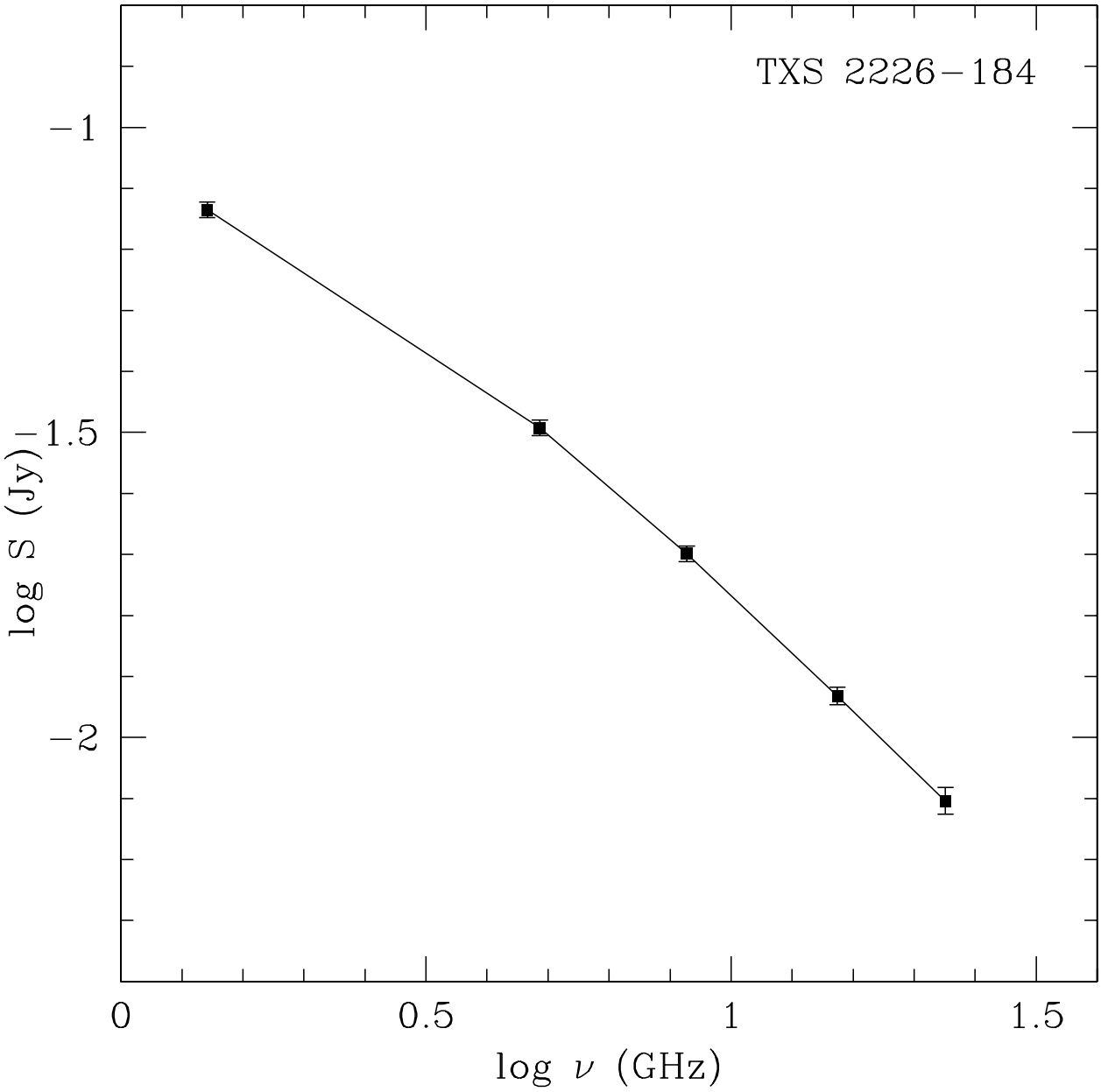

Fig. 4.— The broadband continuum emission spectrum towards TXS 2226-184 derived from observations in April 2001.

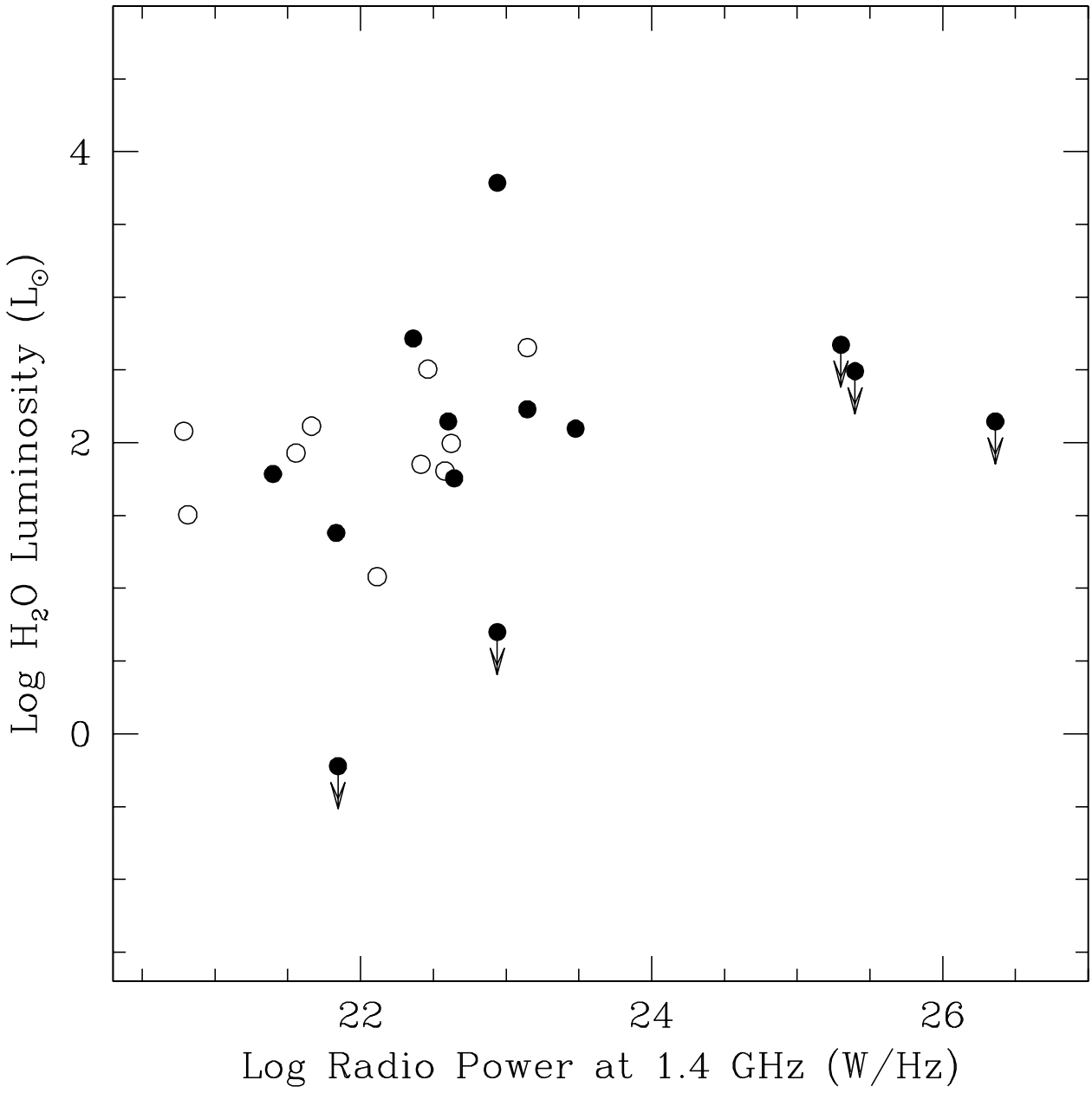

Fig. 5.— A plot of H_2O Maser Luminosity against the Radio Power at an observed frequency of 1.4 GHz for all the sources in Table 1. Sources plotted with filled circles have HI detected in absorption, while those plotted with empty circles have either not been detected or not been observed.